ACS APPLIED MATERIALS & INTERFACES

Letter

www.acsami.org

Enhancing the Photovoltaic Performance by Tuning the Morphology of Polymer:$PC_{71}BM$ Blends with a Commercially Available Nucleating Agent

Heng Lu,[†] Yang Wu,[‡] Wenhua Li,*[,†] Hedi Wei,[†] Wei Ma,*[,‡] and Zhishan Bo*[,†]

[†]Beijing Key Laboratory of Energy Conversion and Storage Materials, College of Chemistry, Beijing Normal University, Beijing 100875, China

[‡]State Key Laboratory for Mechanical Behavior of Materials, Xi'an Jiaotong University, Xi'an 710049, China

Supporting Information

ABSTRACT: The use of a commercially available nucleating agent as the additive for the fabrication of polymer:$PC_{71}BM$-based active layers by solution-processing can greatly enhance the power conversion efficiency (PCE) of bulk heterojunction polymer solar cells (BHJ PSCs). The enhancement of device performance is mainly due to the addition of nucleating agent, which is able to regulate the drying process of the active layer and decrease the oversized domain size of conjugated polymers. Via this effective strategy to optimize the film morphology, the designed device exhibits an enhancement as great as 30.8%.

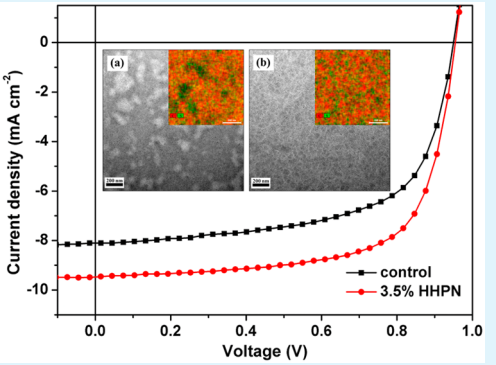

KEYWORDS: *polymer solar cells, nucleating agent, morphology control, domain size, conjugated polymers*

As one of the most efficient devices with remarkable advantages,[1−7] bulk heterojunction polymer solar cells (BHJ PSCs) possess great potential for enhancing the power conversion efficiency (PCE). This "potential" has recently brought up the value of PCE as high as 11% by designing new conjugated polymers and adjusting the morphology of active layer.[8,9] Tremendous efforts have been put forward to synthesize new conjugated polymers and to study the relationship between the morphology of active layer and device efficiency.[8,10−12] The active layer of PSCs is a blend of polymer donor and phenyl C_{71}-butyric acid methyl ester ($PC_{71}BM$) acceptor, it is essential to keep the polymer domain size less than 20 nm in order to guarantee the efficient diffusion of the photogenerated excitons over the donor/acceptor (D/A) interfaces within the decay time.[13] Furthermore, more heterojunction sites formed in D/A interfaces are favorable to efficiently dissociate the excitons into free charge carriers. A bicontinuous interpenetrating network is beneficial for charge transport and collection.[14,15] To optimize the morphology of active layer, different strategies such as thermal annealing, solvent vapor annealing, and the addition of cosolvent or various additives including small molecules,[16,17] polymers,[18−22] inorganic nanocrystals,[23,24] etc. have been developed. Utilizing an additive in the processing solvent, which can influence the drying process of blend film, is the mostly used method to control the morphology of active layer. For examples, 1,8-diiodooctane (DIO) and 1-chloronaphthalene (1-CN) are commonly adopted additives in tuning the morphology of active layers. Although, these additives can effectively enhance the performance of PSCs, as high boiling point solvents the completely removal of DIO or 1-CN under high vacuum requires a quite long time, which makes the practical production of large area devices more complicated. Herein, we report the enhancement of the performance of BHJ PSCs by using a commercially available nucleating agent (Hyperform HPN-68L, simply abbreviated as HHPN) as an additive for solution-processing the active layer and discuss the possible mechanism of tuning the morphology of blend films. HHPN is a commercially available nucleating agent used for tuning the morphology of polyolefin resins, it can usually promote the crystallization speed, enhance the crystallinity, and control the crystal form. The great advantage of using nucleating agent over other methods mentioned above to regulate the morphology of active layer is the simplicity in device processing. To the best of our knowledge, this is the first report of using a commercially available nucleating agent in controlling the morphology of active layers of PSCs to achieve improved device performance.

As shown in Scheme 1, the bulk heterojunction photovoltaic device is constructed in a configuration of ITO/PEDOT:PSS (35 nm)/active layer (~100 nm)/LiF (0.6 nm)/Al (100 nm). Detailed information on the particular fabrication conditions is

Received: July 22, 2015
Accepted: August 19, 2015

DOI: 10.1021/acsami.5b06674
ACS Appl. Mater. Interfaces XXXX, XXX, XXX−XXX

Scheme 1. Device Structure and Chemical Structures of Donor and Acceptor

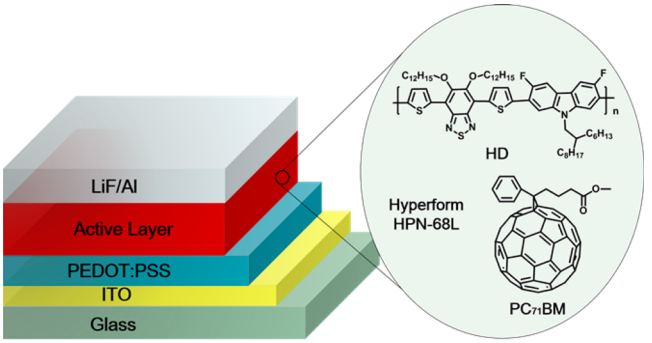

included in the Supporting Information. The homemade polymer poly[3,6-difluoro-9-hexyldecyl-9H-2,7-carbazole-*alt*-5,5-(4′,7′-di-2-thienyl-5′,6′-bis(dodecyloxy)-2′,1′,3′-benzothiadiazole)] (HD-PDFCDTBT, simply abbreviated as HD) in combination with $PC_{71}BM$ was selected as the active layer components and their structures are presented in the inset of Scheme 1. Moreover, HD was used as a high efficiency electron donor material in our previous study.[25] UV−visible absorption spectrum (Figure S1) of the polymer film exhibits three peaks appearing at 410, 538, and 578 nm, respectively, and the absorption range is mainly located in the region from 500 to 600 nm. To examine the influence of nucleating agent on the optical properties of active layers, we have fabricated HD:$PC_{71}BM$ blend films without and with the nucleating agent HHPN. Blend films containing the nucleating agent were fabricated by spin-coating from a solution of HD, $PC_{71}BM$, and HPPN in 1,2-dichlorobenzene (DCB). The blend films without or with HHPN nucleating agent exhibited similar absorption spectra, suggesting that the nucleating agent does not affect the optical property of the active layer.

The representative current−voltage (J−V) characteristics of devices fabricated without and with 3.5 wt % HHPN under white light illumination are shown in Figure 1a, and their photovoltaic performances including the J_{sc}, open-circuit voltage (V_{oc}), fill factor (FF), and the final PCE values are summarized in Table 1. The value of PCE for the plain devices fabricated under the optimal condition is ca. 4.74%, which is comparable with the reported result,[25] and the J_{sc} is 8.00 mA cm^{-2}. This parameter dramatically increases for devices fabricated from spin-coating a blend solution containing a small amount of nucleating agent. Distinct difference for the J−V curves of devices processed from DCB without and with 3.5 wt % HHPN is observed. After the addition of 3.5 wt % HHPN as the additive, all device parameters were simultaneously improved. The J_{sc} was enhanced to 9.50 mA cm^{-2} and the FF showed an improvement of 9.6% (from 0.63 to 0.68). Therefore, the maximum PCE of 6.2% and a significant enhancement of 30.8% over the plain device (0 wt % HHPN) are mainly assigned to the combined contributions devoted by both the J_{sc} and FF, even though it is due in large part to a higher J_{sc} with the improvement of 18.8%.

Different amounts of HHPN and various additives are employed so as to better understand the influence of HHPN on the solar cell efficiency. As depicted in Table S1 and Table 1, devices containing the optimal amount of HHPN (3.5 wt %) exhibit the highest J_{sc}, V_{oc}, and FF compared to the values of films with less (1.0 wt %) or more (5.5 wt %) HHPN and they rank first as well in the measured J_{sc} and V_{oc} compared to films spin-coated with other processing additives like 1-CN and DIO. Hence, the utilization of HHPN is an effective strategy for improving the PCE of PSCs and its optimized content is crucial to achieve the most efficient devices. To verify the J_{sc} value obtained from J−V measurements, external quantum efficiencies (EQEs) of devices without and with 3.5 wt % HHPN were measured. As shown in Figure 1b, the EQE value of HHPN-based devices is much higher than that of the plain devices. In addition, the J_{sc} values obtained from J−V measurements fit very well with that calculated by the integration of EQE curves, indicating that the obtained PCEs are very believable.

As the most key parameters in determining the PCE of BHJ devices, J_{sc} and FF values are closely correlated to the morphology of active layer. Therefore, the influence of HHPN on the morphology of active layer was investigated by Grazing incident wide-angle X-ray scattering (GIWAXS) and resonant soft X-ray scattering (R-SoXS). GIWAXS was used to gain insight into the crystallinity of blend films processed with or without HHPN (Figure 2). The molecular packing orientation can be deduced from the GIWAXS patterns, where the molecular packing out-of-plane appears nominally along the q_z axis and the in-plane ordering along the q_{xy}. No clear (h00) peaks are observed in the blends processed with or without HHPN, indicating that HD is most likely amorphous. The diffraction peak at $q \approx 1.4$ $Å^{-1}$ is generated from PCBM aggregation. The weak π−π stacking peaks emerge at $q \approx 1.8$ $Å^{-1}$. The slightly higher (010) π−π stacking suggests that HHPN improves the polymer π−π stacking ordering in the blends.

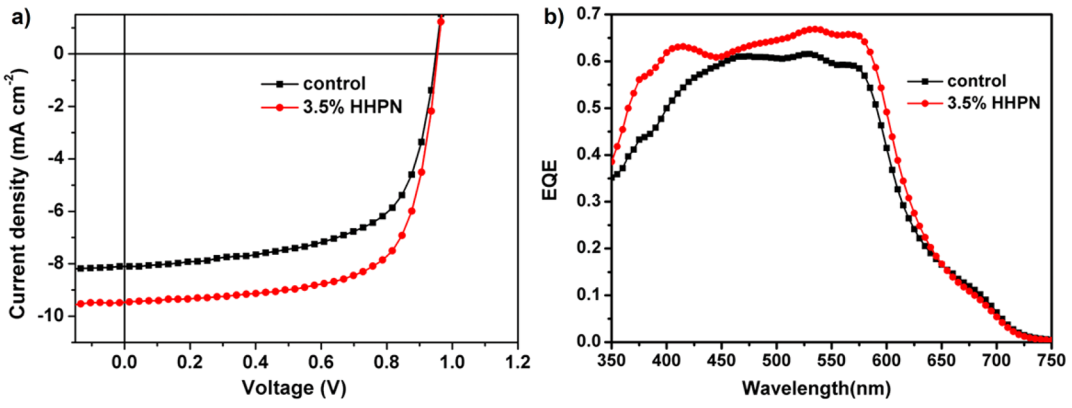

Figure 1. (a) J−V characteristics of devices measured under the illumination of AM 1.5 G (100 mW cm^{-2}) from a solar simulator; (b) EQE curves.

DOI: 10.1021/acsami.5b06674
ACS Appl. Mater. Interfaces XXXX, XXX, XXX−XXX

Table 1. Parameters of BHJ Solar Cells

additive	FF	V_{oc} (V)	J_{sc}[a] (mA cm^{-2})	PCE[b] (%)	R_s (Ω cm^2)	μ_h (cm^2 V^{-1} s^{-1})
without	0.63	0.95	8.47	4.88 (4.78)	11.62	2.56×10^{-4}
3.5 wt % HHPN	0.68	0.96	9.50	6.20 (6.06)	7.81	5.90×10^{-4}
3 vol % 1-CN	0.73	0.94	7.82	5.43 (5.30)	10.49	1.75×10^{-4}
2 vol % DIO	0.56	0.91	9.25	5.38 (5.33)	8,62	3.79×10^{-4}

[a]J_{sc} was calculated by integrating the EQE spectrum with the AM 1.5G spectrum. [b]The average PCE was in bracket and obtained from over 5 devices.

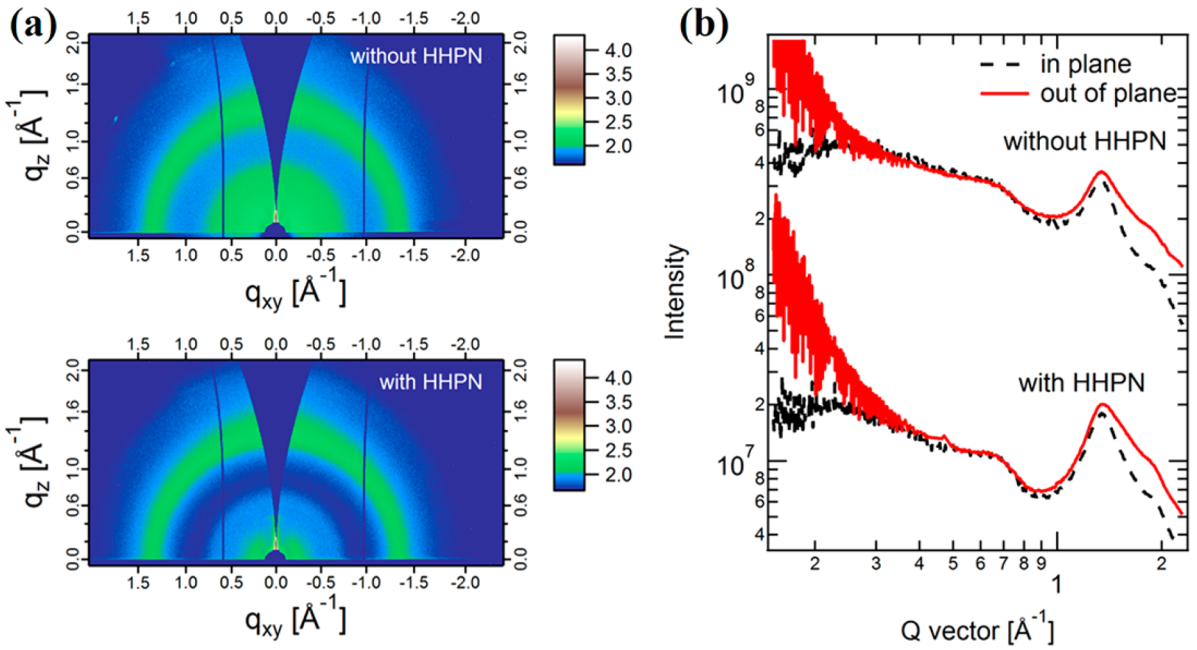

Figure 2. (a) GIWAXS 2D pattern of the blend processed with and without HHPN as additive; (b) scattering profiles of in-plane and out-of-plane.

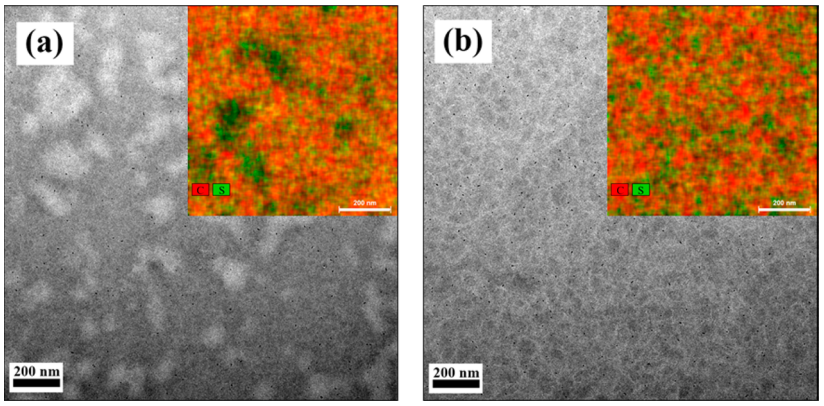

Figure 3. Bright-field TEM images of active layer (polymer:fullerene) spin-cast from DCB (a) without any additive and (b) with 3.5 wt % HHPN. Insert graphs are electron energy loss spectroscopy (EELS) elemental mapping images, C (red dots) and S mapping (green dots) of optimum BHJ film prepared from DCB. Scale bar of EELS mapping is 200 nm.

In Figure 3 the bright-field TEM images show the different morphology of active layers spin coated from the blend solution without (a) and with (b) HHPN additives. The seriously aggregated polymer-enriched regions shown as brighter and fullerene-enriched regions as darker are clearly observed in Figure 3a. In this condition, the size of these two kind domains clearly exceeds the exciton diffusion length and the morphology with large pure phase in the mesoscale is formed leading to the coarse phase separation. After the addition of HHPN, instead of the polymer agglomerations, a thin fibrillar network is formed as shown in Figure 3b. This polymer network efficiently restricts the PCBM domains within the nanoscale matrix which makes them dispersive and oriented in a relatively discrete way. In this case, the interpenetrating network structure in the active layer is built which can be further confirmed by the homogeneous distributions of both polymer (green) and $PC_{71}BM$ as depicted in electron energy loss spectroscopy (EELS) elemental mapping images (the insets in the Figure 3). From the X-ray photoelectron spectra (XPS) shown in Figure S2, it is worthy to point out that the evenly distributed element

DOI: 10.1021/acsami.5b06674
ACS Appl. Mater. Interfaces XXXX, XXX, XXX−XXX

S is exclusively derived from the polymer HD because of the absence of element S in HHPN and $PC_{71}BM$. It is notable that the conjugated polymer HD is an amorphous polymer, it prone to form large amorphous aggregates during spin-coating. After the addition of HHPN as the additive, the nucleating agent can probably induce the crystallization (or aggregation) of polymer chains to form fibrillar aggregates and prevent the undesired liquid−liquid phase separation to form large aggregates.[12] Meanwhile, by analyzing AFM images showing in Figure S3, it evidently demonstrates the smoother film obtained in the presence of HHPN and the roughness of the active layer films decreases from 1.12 to 0.88 nm. This is well consistent with the TEM results discussed above. No large $PC_{71}BM$ domains occurring and the remarkably decreased size for fullerene domains boost the formation of bicontinuous percolation pathways which accelerate both the exciton dissociation and the carrier transport. The above-discussed points can be revisited in the context of the EQE measurements, which indicate the improved charge collection upon the addition of HHPN in the active layer.

The phase-separated morphologies of the blends under the different conditions were further investigated by resonant soft X-way scattering (R-SoXS).[26−28] A photon energy of 284.2 eV was selected to provide high polymer/fullerene contrast. Figure 4 shows the R-SoXS profiles for the HD:$PC_{71}BM$ (1:2, w/w) blend films processed with or without HHPN. The scattering profiles represent the distribution function of spatial frequency, s ($s = q/2\pi$), of the samples and are dominated by log-normal distributions that can be fitted by a set of Gaussians in lin-log space. The median of the distribution s_{median} corresponds to the characteristic median length scale, ξ, of the corresponding log-normal distribution in real space with $\xi = 1/s_{median}$, a model independent statistical quantity. When the blend films were processed without HHPN, the profile showed a scattering intensity with a ξ of ∼30−40 nm; when HHPN was used as an additive, the scattering profile showed a decreased ξ of ∼20−30 nm. These results are consistent with the TEM and AFM results. The average composition variation (and relative domain purity) can also be revealed by R-SoXS via integration of the scattering profiles.[27] Completely mixed domains result in no scattering over the q-range probed. A two phase morphology with pure phases will yield maximum scattering. Intermediate scattering intensity reflects the average composition of all domain of a two or likely three phase morphology. The relative domain purity for blends processed without and with HHPN are 92 and 100%. The smaller and purer domains obtained by processed with HHPN are favorable for exciton dissociation efficiency and for reduced bimolecular recombination. This leads to the enhanced J_{sc} and FF.[29]

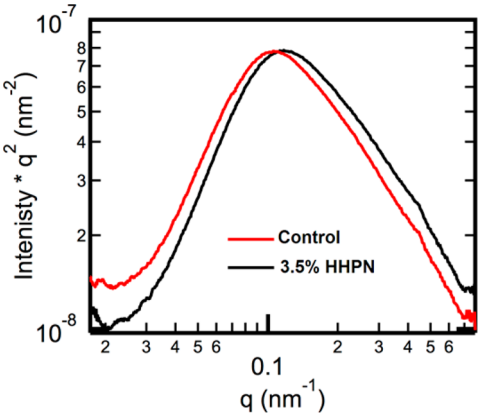

Figure 4. R-SoXS profiles for the blend films of HD:$PC_{71}BM$ (1:2, w/w) with or without HHPN.

To further elucidate the effect of HHPN additive on the charge transport, we measured the hole and electron mobility of BHJ PSCs by space charge limited current (SCLC) method. The hole-only diode is fabricated in a device configuration: ITO/PEDOT:PSS/HD:$PC_{71}BM$/Au and electron-only diode with a device configuration: FTO/HD:$PC_{71}BM$/Al. The transfer characteristic curves are shown in Figure 5a and Figure S4. Hole and electron mobilities are calculated according to equations reported in the literature.[30,31] As illustrated in Table 1, the hole mobility of devices fabricated with 3.5 wt % HHPN reached 5.90×10^{-4} cm^2 V^{-1} s^{-1}, which is two times higher than that of plain devices, suggesting the benefits for charge transport conferred by the improved morphology of fibrillar network. Meanwhile, the series resistance (R_s) of PSCs can be obtained from the inverse slope of the dark $J-V$ curve (Figure 5b). The R_s value declines remarkably from 11.62 to 7.81 Ω cm^2 with the addition of HHPN, which coincides well with higher short-circuit currents and improved charge transport.

In conclusion, HD:$PC_{71}BM$-based BHJ PSCs with enhanced photovoltaic performance are developed by incorporation of a commercial available nucleating agent HHPN in the active layer. The designed devices exhibit an overall PCE as high as 6.20% and the enhancements of 30.8% originated from both

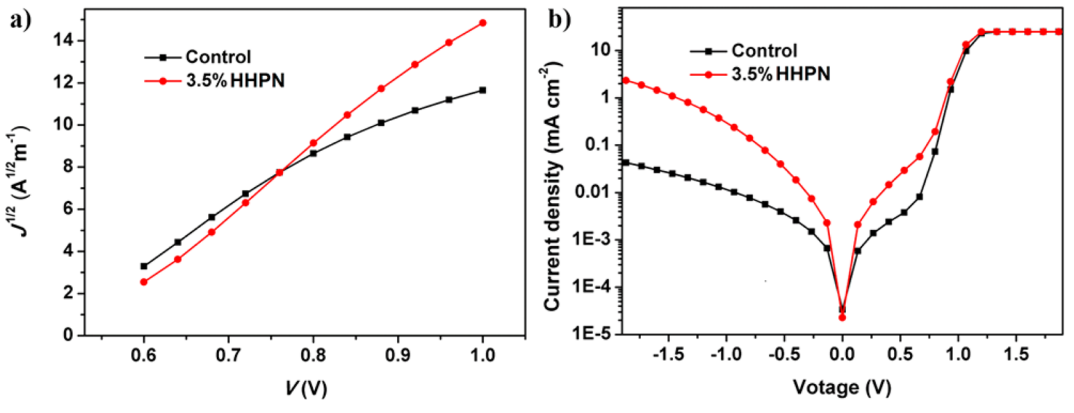

Figure 5. $J-V$ characteristics under dark for (a) hole-only devices; (b) dark $J-V$ curves.

DOI: 10.1021/acsami.5b06674
ACS Appl. Mater. Interfaces XXXX, XXX, XXX−XXX

the greatly improved J_{sc} and FF. The enhancement of device performance is mainly due to that the addition of nucleating agent can regulate the drying process of active layer and decrease the oversized domain size of conjugated polymers. Our study also demonstrates that HHPN is a more effective additive over other most used additives such as 1-CN and DIO to achieve higher photovoltaic performance. Considering the easy processability and the commercial availability, the addition of nucleating agent maybe used as an alternative choice in device fabrication, especially for the practical large area processing.

■ ASSOCIATED CONTENT

Supporting Information

The Supporting Information is available free of charge on the ACS Publications website at DOI: 10.1021/acsami.5b06674.

General measurements and characterization; fabrication of polymer solar cells; UV−vis absorption spectra of polymer and blend films; the XPS data of HHPN; AFM height images of the blend film(PDF)

■ AUTHOR INFORMATION

Corresponding Authors

*E-mail: liwenhua@bnu.edu.cn.
*E-mail: msewma@mail.xjtu.edu.cn.
*E-mail: zsbo@bnu.edu.cn.

Notes

The authors declare no competing financial interest.

■ ACKNOWLEDGMENTS

The authors thank for the financial support by the NSF of China (91233205 and 21421003) and Beijing Natural Science Foundation (2132042). Thanks Dr. Dong Zheng (Beijing Normal University) and Dr. Dongchang Wu (FEI Company Shanghai Nanoport) for the assistance in HRTEM measurements. X-ray data was acquired at beamlines 11.0.1.2 and 7.3.3 at the Advanced Light Source, which is supported by the Director, Office of Science, Office of Basic Energy Sciences, of the U.S. Department of Energy under Contract DE-AC02-05CH11231.

■ REFERENCES

(1) Kim, J. Y.; Lee, K.; Coates, N. E.; Moses, D.; Nguyen, T.-Q.; Dante, M.; Heeger, A. J. Efficient Tandem Polymer Solar Cells Fabricated by All-Solution Processing. *Science* **2007**, *317*, 222−225.

(2) Minnaert, B.; Burgelman, M. Efficiency Potential of Organic Bulk Heterojunction Solar Cells. *Prog. Photovoltaics* **2007**, *15*, 741−748.

(3) Thompson, B. C.; Fréchet, J. M. J. Polymer−Fullerene Composite Solar Cells. *Angew. Chem., Int. Ed.* **2008**, *47*, 58−77.

(4) Ameri, T.; Dennler, G.; Lungenschmied, C.; Brabec, C. J. Organic Tandem Solar Cells: A Review. *Energy Environ. Sci.* **2009**, *2*, 347−363.

(5) Chen, J.; Cao, Y. Development of Novel Conjugated Donor Polymers for High-Efficiency Bulk-Heterojunction Photovoltaic Devices. *Acc. Chem. Res.* **2009**, *42*, 1709−1718.

(6) Cheng, Y.-J.; Yang, S.-H.; Hsu, C.-S. Synthesis of Conjugated Polymers for Organic Solar Cell Applications. *Chem. Rev.* **2009**, *109*, 5868−5923.

(7) He, Z.; Zhong, C.; Su, S.; Xu, M.; Wu, H.; Cao, Y. Enhanced Power-Conversion Efficiency in Polymer Solar Cells Using an Inverted Device Structure. *Nat. Photonics* **2012**, *6*, 591−595.

(8) Liu, Y.; Zhao, J.; Li, Z.; Mu, C.; Ma, W.; Hu, H.; Jiang, K.; Lin, H.; Ade, H.; Yan, H. Aggregation and Morphology Control Enables Multiple Cases of High-Efficiency Polymer Solar Cells. *Nat. Commun.* **2014**, *5*, 5293−5300.

(9) He, Z.; Xiao, B.; Liu, F.; Wu, H.; Yang, Y.; Xiao, S.; Wang, C.; Russell, T. P.; Cao, Y. Single-Junction Polymer Solar Cells with High Efficiency and Photovoltage. *Nat. Photonics* **2015**, *9*, 174−179.

(10) Lyons, B. P.; Clarke, N.; Groves, C. The Relative Importance of Domain Size, Domain Purity and Domain Interfaces to the Performance of Bulk-Heterojunction Organic Photovoltaics. *Energy Environ. Sci.* **2012**, *5*, 7657−7663.

(11) Kouijzer, S.; Michels, J. J.; van den Berg, M.; Gevaerts, V. S.; Turbiez, M.; Wienk, M. M.; Janssen, R. A. Predicting Morphologies of Solution Processed Polymer:Fullerene Blends. *J. Am. Chem. Soc.* **2013**, *135*, 12057−12067.

(12) van Franeker, J. J.; Turbiez, M.; Li, W.; Wienk, M. M.; Janssen, R. A. A Real-Time Study of the Benefits of Co-Solvents in Polymer Solar Cell Processing. *Nat. Commun.* **2015**, *6*, 6229−6236.

(13) Mikhnenko, O. V.; Azimi, H.; Scharber, M.; Morana, M.; Blom, P. W. M.; Loi, M. A. Exciton Diffusion Length in Narrow Bandgap Polymers. *Energy Environ. Sci.* **2012**, *5*, 6960−6965.

(14) Guo, J.; Ohkita, H.; Benten, H.; Ito, S. Charge Generation and Recombination Dynamics in Poly(3-hexylthiophene)/Fullerene Blend Films with Different Regioregularities and Morphologies. *J. Am. Chem. Soc.* **2010**, *132*, 6154−6164.

(15) Heeger, A. J. 25th Anniversary Article: Bulk Heterojunction Solar Cells: Understanding the Mechanism of Operation. *Adv. Mater.* **2014**, *26*, 10−28.

(16) Chan, S.-H.; Lai, C.-S.; Chen, H.-L.; Ting, C.; Chen, C.-P. Highly Efficient P3HT: C60 Solar Cell Free of Annealing Process. *Macromolecules* **2011**, *44*, 8886−8891.

(17) Seri, M.; Marrocchi, A.; Bagnis, D.; Ponce, R.; Taticchi, A.; Marks, T. J.; Facchetti, A. Molecular-Shape-Controlled Photovoltaic Performance Probed Via Soluble Pi-Conjugated Arylacetylenic Semiconductors. *Adv. Mater.* **2011**, *23*, 3827−3831.

(18) Yang, C.; Lee, J. K.; Heeger, A. J.; Wudl, F. Well-Defined Donor-Acceptor Rod-Coil Diblock Copolymers Based on P3HT Containing C60: the Morphology and Role As a Surfactant in Bulk-Heterojunction Solar Cells. *J. Mater. Chem.* **2009**, *19*, 5416−5423.

(19) Tsai, J.-H.; Lai, Y.-C.; Higashihara, T.; Lin, C.-J.; Ueda, M.; Chen, W.-C. Enhancement of P3HT/PCBM Photovoltaic Efficiency Using the Surfactant of Triblock Copolymer Containing Poly(3-hexylthiophene) and Poly(4-vinyltriphenylamine) Segments. *Macromolecules* **2010**, *43*, 6085−6091.

(20) Chang, S.-Y.; Liao, H.-C.; Shao, Y.-T.; Sung, Y.-M.; Hsu, S.-H.; Ho, C.-C.; Su, W.-F.; Chen, Y.-F. Enhancing the Efficiency of Low Bandgap Conducting Polymer Bulk Heterojunction Solar Cells Using P3HT As a Morphology Control Agent. *J. Mater. Chem. A* **2013**, *1*, 2447−2452.

(21) Graham, K. R.; Stalder, R.; Wieruszewski, P. M.; Patel, D. G.; Salazar, D. H.; Reynolds, J. R. Tailor-Made Additives for Morphology Control in Molecular Bulk-Heterojunction Photovoltaics. *ACS Appl. Mater. Interfaces* **2013**, *5*, 63−71.

(22) Li, A.; Amonoo, J.; Huang, B.; Goldberg, P. K.; McNeil, A. J.; Green, P. F. Enhancing Photovoltaic Performance Using an All-Conjugated Random Copolymer to Tailor Bulk and Interfacial Morphology of the P3HT:ICBA Active Layer. *Adv. Funct. Mater.* **2014**, *24*, 5594−5602.

(23) Liao, H.-C.; Tsao, C.-S.; Lin, T.-H.; Jao, M.-H.; Chuang, C.-M.; Chang, S.-Y.; Huang, Y.-C.; Shao, Y.-T.; Chen, C.-Y.; Su, C.-J.; Jeng, U. S.; Chen, Y.-F.; Su, W.-F. Nanoparticle-Tuned Self-Organization of a Bulk Heterojunction Hybrid Solar Cell with Enhanced Performance. *ACS Nano* **2012**, *6*, 1657−1666.

(24) Li, S.; Li, W.; Liu, Q.; Wei, H.; Jin, E.; Wang, H.; Dong, Y.; Lu, H.; Zhang, X.; Zhao, X.; Wang, M.; Bo, Z. Spin-coated Ag Nanoparticles onto ITO Substrates for Efficient Improvement of Polymer Solar Cell Performance. *J. Mater. Chem. C* **2015**, *3*, 1319−1324.

(25) Wei, H.; Chao, Y.-H.; Kang, C.; Li, C.; Lu, H.; Gong, X.; Dong, H.; Hu, W.; Hsu, C.-S.; Bo, Z. High-Efficiency Large-Bandgap Material for Polymer Solar Cells. *Macromol. Rapid Commun.* **2015**, *36*, 84−89.

(26) Collins, B. A.; Cochran, J. E.; Yan, H.; Gann, E.; Hub, C.; Fink, R.; Wang, C.; Schuettfort, T.; McNeill, C. R.; Chabinyc, M. L.; Ade, H.

DOI: 10.1021/acsami.5b06674
ACS Appl. Mater. Interfaces XXXX, XXX, XXX−XXX

Polarized X-ray Scattering Reveals Non-Crystalline Orientational Ordering in Organic Films. *Nat. Mater.* **2012**, *11*, 536−543.
(27) Ma, W.; Tumbleston, J. R.; Wang, M.; Gann, E.; Huang, F.; Ade, H. Domain Purity, Miscibility, and Molecular Orientation at Donor/Acceptor Interfaces in High Performance Organic Solar Cells: Paths to Further Improvement. *Adv. Energy Mater.* **2013**, *3*, 864−872.
(28) Ma, W.; Tumbleston, J. R.; Ye, L.; Wang, C.; Hou, J.; Ade, H. Quantification of Nano- and Mesoscale Phase Separation and Relation to Donor and Acceptor Quantum Efficiency, J(sc), and FF in Polymer:Fullerene Solar Cells. *Adv. Mater.* **2014**, *26*, 4234−4241.
(29) Albrecht, S.; Janietz, S.; Schindler, W.; Frisch, J.; Kurpiers, J.; Kniepert, J.; Inal, S.; Pingel, P.; Fostiropoulos, K.; Koch, N.; Neher, D. Fluorinated Copolymer PCPDTBT with Enhanced Open-Circuit Voltage and Reduced Recombination for Highly Efficient Polymer Solar Cells. *J. Am. Chem. Soc.* **2012**, *134*, 14932−14944.
(30) Goh, C.; Kline, R. J.; McGehee, M. D.; Kadnikova, E. N.; Fréchet, J. M. J. Molecular-Weight-Dependent Mobilities in Regioregular Poly(3-hexyl-thiophene) Diodes. *Appl. Phys. Lett.* **2005**, *86*, 122110−122113.
(31) Koppe, M.; Egelhaaf, H. J.; Dennler, G.; Scharber, M. C.; Brabec, C. J.; Schilinsky, P.; Hoth, C. N. Near IR Sensitization of Organic Bulk Heterojunction Solar Cells: Towards Optimization of the Spectral Response of Organic Solar Cells. *Adv. Funct. Mater.* **2010**, *20*, 338−346.

DOI: 10.1021/acsami.5b06674
ACS Appl. Mater. Interfaces XXXX, XXX, XXX−XXX